Chemical routes to oxides: alkoxide *vs.* alkoxide–acetate routes: synthesis, characterization, reactivity and polycondensation of $MNb_2(OAc)_2(OPr^i)_{10}$ (M = Mg, Cd, Pb) species

Souad Boulmaâz,[a] Renée Papiernik,[a] Liliane G. Hubert-Pfalzgraf*,[a] Bernard Septe[a] and Jacqueline Vaissermann[b]

[a]*Laboratoire de Chimie Moléculaire, URA-CNRS, Université de Nice-Sophia Antipolis, 06108 Nice Cédex 2, France*
[b]*Laboratoire de Chimie des Métaux de Transition, URA-CNRS, 75230 Paris Cédex, France*

The molecular constitution of solutions containing niobium alkoxides and divalent metal acetates $M(OAc)_2$ (M = Mg, Ba, Pb, Zn, Cd) has been examined. The heterometallic aggregates $MNb_2(\mu\text{-}OAc)_2(\mu\text{-}OPr^i)_4(OPr^i)_6$ (M = Mg **1**, Cd **2**, Pb **3a**) have been isolated and characterized by elemental analysis, FTIR, multinuclear NMR (^1H, ^{13}C, ^{207}Pb, ^{113}Cd) and by single-crystal X-ray diffraction for M = Mg and Cd. The magnesium derivative crystallizes in the monoclinic system, space group $P2_1/c$ with the unit-cell parameters $a = 21.238(5)$, $b = 10.127(10)$, $c = 24.861(3)$ Å, $\beta = 107.77(2)^\circ$ and $Z = 4$. The thermal stability of the various species has been investigated. Condensation is induced thermally for $PbNb_2(OAc)_2(OPr^i)_{10}$. The reactivity between $MNb_2(\mu\text{-}OAc)_2(\mu\text{-}OPr^i)_4(OPr^i)_6$ (M = Pb, Mg) and other metallic species has been evaluated. A terheterometallic compound, $PbMgNb_2O(OAc)_2(OPr^i)_{10}$ has been isolated. Whereas no reaction is observed between $Ba(OAc)_2$ and $Nb(OPr^i)_5$, the reaction between metal alkoxides affords $BaNb_2(OPr^i)_{12}(Pr^iOH)_2$. Its reactivity shows that the absence of an assembling acetate ligand induces facile separation between the metals. Results of the hydrolysis experiments of **1**–**3a** are given. The powders have been analyzed by TG, SEM–EDX, light scattering and XRD. The merit of the assembling acetate ligand for avoiding the segregation of the metals is emphasized.

Mixed-metal oxides represent an important class of advanced materials due to their palette of technological applications.[1] Their uses include catalysts and structural ceramics, but they have mostly been acclaimed for their applications as sensors, actuators and smart materials.[2] Techniques for the formation of such materials, including chemical vapor deposition (CVD), sol–gel processes, metal–organic decomposition and molecular beam epitaxy, to name a few, require metal–organic molecules which have specific physical and chemical properties, as precursors. The preparation of inorganic materials from metal–organic precursors generally has the advantages over 'traditional routes' of low temperatures of formation and/or crystallization, better compositional uniformity and conformal coverage in the case of films.[3] Metal alkoxides $M(OR)_n$ or oxoalkoxides $MO(OR)_n$ are versatile molecular precursors of metal oxides, one of their most attractive features being their solubility in a large variety of solvents and their ability to form heterometallic species, especially by mixing alkoxides of different metals.[4] However, to overcome the difficulty in handling alkoxides and/or in their availability, more commonly accessible derivatives such as carboxylates (often acetates), nitrates, halides, hydroxides or β-diketonates have often been used in conjunction with metal alkoxides. The molecular constitution of such solutions is almost unknown, although a better understanding could allow a better control of the hydrolysis–polymerization process and thus of the properties of the resulting material.

We report here the results of the investigations of the $M(OAc)_2$–$Nb(OR)_5$ (M = Mg, Ba, Zn, Cd, Pb) systems. Insight into the molecular composition of homogeneous solutions has been gained by using a variety of spectroscopic techniques, IR and nuclear magnetic resonance (^1H and ^{13}C as well as metal NMR, namely ^{207}Pb or ^{113}Cd), and in the most favorable cases by single-crystal X-ray diffraction. The heterometallic species $MNb_2(\mu\text{-}OAc)_2(\mu\text{-}OR)_4(OR)_6$ (M = Mg, Cd; R = Pr^i) have thus been unequivocally characterized. Their reactivity as well as that of a Ba–Nb species having a similar stoichiometry, $BaNb_2(OPr^i)_{12}(Pr^iOH)_2$ has been examined. The transformation of the acetatoalkoxides by hydrolysis–polycondensation reactions has been achieved. Results on the Nb–Cd system have been reported in a communication.[5]

Experimental

All manipulations were routinely performed under nitrogen atmosphere using Schlenk tubes and vacuum line techniques with dried and distilled solvents. Niobium[6] and lead alkoxides,[7] $BaNb_2(OPr^i)_{12}(Pr^iOH)_2$,[8] lead[9] and zinc[10] trimethylsilylamides were prepared according to the literature. Anhydrous metal acetates were obtained by refluxing metal acetate hydrates with acetic anhydride over 15 h. ^1H, ^{13}C, ^{113}Cd and ^{207}Pb NMR spectra were recorded on solutions (concentrations: 1 M for ^{113}Cd and 0.3 M for ^{207}Pb) on a Bruker AC-200 spectrometer. The chemical shifts are reported with respect to $M(NO_3)_2$ (M = Cd, Pb) in aqueous solutions as external references, they are positive to low fields. IR spectra were registered with a FT–IRS 45 Bruker spectrometer as Nujol mulls between KBr plates for the air-sensitive derivatives and as KBr pellets for the powders resulting from hydrolysis. Analytical data were obtained from the Centre de Microanalyses du CNRS. IR and NMR data are listed in Table 1.

Hydrolyses were achieved at room temperature in THF or isopropyl alcohol (0.1–0.05 M) without additives, the water being added *via* these solvents. The powders were characterized by TG–DTA with a Setaram system (nitrogen, heating rate of 5 °C min^{-1}). Powder X-ray diffraction patterns were collected using Cu-Kα radiation after calcination at various temperatures.

Synthesis of $MgNb_2(OAc)_2(OPr^i)_{10}$ 1

Anhydrous $Mg(OAc)_2$ (1 g, 7.02 mmol) was added to a solution of $Nb(OPr^i)_5$ (5.02 g, 12.94 mmol) in 25 ml of hexane (or toluene) at room temperature. After stirring for 1 to 2 h, the excess of $Mg(OAc)_2$ was eliminated by filtration. Crystallization was achieved at 5 °C (5.88 g, 99%). Anal. Calc. for

Table 1 IR and NMR (^{1}H, ^{13}C, ^{207}Pb) spectroscopic data for mixed-metal acetatoalkoxides

	IR/cm^{-1}		NMR (25 °C, δ $CDCl_3$)[a]						
			^{207}Pb, $^{113}Cd\{^{1}H\}$	^{1}H				$^{13}C\{^{1}H\}$	
compound	νCO_2	νMOZ (Z = Ac, Et, Pr^{i})	(toluene)	CH_3(Ac)	CH_2(Et), CH (Pr)	CH_3 (Et, Pr^{i})	CO(Ac)	CH_2(Et), CH (Pr^{i})	CH_3 (Et, Pr^{i}, Ac)
$MgNb_2(OAc)_2(OPr^{i})_{10}$ **1**	1590vs, 1429vs	662m, 616w, 581m, 564m, 529m, 478s, 391m	—	1.90 (s,3H)	4.75, 4.67, 4.54 (spt, 2:2:1, 5H)	1.33, 1.30, 1.20 (d, 2:2:1, 30H)	177.4	75.4, 75.3 71.8, 70.6	25.8, 25.4, 24.6, 24.2
$CdNb_2(OAc)_2(OPr^{i})_{10}$ **2**	1574vs, 1423s	579s, 557(sh), 518w, 446s	33.8	1.95 (s,3H)	4.70 (spt, 5H)	1.28 (d, 30H)	177.6	74.1	25.4, 24.7
$PbNb_2(OAc)_2(OPr^{i})_{10}$ **3a**	1560vs, 1415vs	659m, 644m, 608(sh), 571vs, 512w, 466m 432m	2390	25 °C: 1.97(s,3H) −50 °C: 1.95(s)	25 °C: 4.99, 4.69 (spt, 3:2, 5H) −50 °C 4.95, 4.83, 4.65 (spt, 2:2:1)	25 °C: 1.27 (d,30H) −50 °C: 1.22 (ov.d)	177.8	74.7, 73.9	25.8, 25.3, 24.6, 23.8
$PbNb_2(OAc)_2(OEt)_{10}$ **3b**	1566vs, 1414m	662s, 555s, 403m	2325	1.75(s,3H)	4.50, 4.30 (q, 2:3, 10H)	1.21 (ov.t, 15H)	178.6	67.2, 62.9	23.7, 20.0, 18.2, 18.1

[a]s = Singlet, d = doublet, q = quartet, spt = septet, m = multiplet, ov.d = overlapping of doublets, ov.t = overlapping of triplets. Coupling constants J = 7 Hz (Et), 6 Hz (Pr^{i}).

$C_{34}H_{76}MgNb_2O_{14}$: C, 44.43; H, 8.27; Mg, 2.64; Nb, 20.23. Found: C, 43.53; H, 8.12; Mg, 2.35; Nb, 20.30%.

Synthesis of $CdNb_2(OAc)_2(OPr^i)_{10}$ 2 and of $PbNb_2(OAc)_2(OR)_{10}$ (R = Pr^i 3a, Et 3b)

Colourless needles were obtained by the same procedure (93%) for **2** and for **3a** (99%). Anal. Calc. for $C_{34}H_{76}CdNb_2O_{14}$: C, 39.23; H, 7.45; Cd, 10.76; Nb, 18.92. Found: C, 38.99; H, 7.17; Cd, 10.82; Nb, 18.74. Anal. Calc. for $C_{34}H_{76}Nb_2O_{14}Pb$: C, 37.05; H, 6.90; Pb, 18.81; Nb, 16.87. Found: C, 36.99; H, 6.87; Pb, 18.79; Nb, 16.85%.

Unit-cell parameters for **3a** (−100 °C): a = 10.308(3), b = 14.114(3), c = 34.121(3) Å, β = 99.08(2)°.

$PbNb_2(OAc)_2(OEt)_{10}$ **3b** was obtained accordingly from $Nb(OEt)_5$ and $Pb(OAc)_2$ in toluene in a 65% yield. Anal. Calc. for $C_{24}H_{56}Nb_2O_{14}Pb$: C, 29.96; H, 5.82; Nb, 19.33; Pb, 21.56. Found: C, 29.36; H, 5.48; Nb, 19.19; Pb, 21.19%.

The various compounds were soluble in common organic solvents including hydrocarbons, **3b** is poorly soluble in ethanol.

Synthesis of $Pb_2Nb_4O_5(OAc)_2(OPr^i)_{12}$ 4

Anhydrous $Pb(OAc)_2$ (0.67 g, 2.06 mmol) was added to a solution of $Nb(OPr^i)_5$ (1.60 g, 4.12 mmol) in 20 ml of toluene and the reaction medium was refluxed for 40 h. After evaporation of the solvent, a yellow oil was obtained. Addition of isopropyl alcohol induced crystallization of thin needles (1.5 g, 86%) which were highly soluble in organic solvents. Anal. Calc. for $C_{40}H_{90}O_{21}Nb_4Pb_2$: C, 28.38, H, 5.36; Nb, 21.95; Pb, 24.47. Found: C, 28.10; H, 5.23; Nb, 22.02; Pb, 24.64%. IR(cm^{-1}): 1570s ($\nu_{as}CO_2$), 1414m (ν_sCO_2); 1160s, 1122s, 1014s, 991s, 960s, 850m, 837m, 826w, 800w (νM−O−M), 663s, 618w; 598s, 569s, 516s, 467m, 430w (νM−OAc, νMOR). ^{1}H NMR ($CDCl_3$, −30 °C): 4.85, 4.69, 4.62 (spt, J = 6 Hz, 1:4:4, 12H, CH), 2.02 (6 H, O Ac), 1.29, 1.22, 1.16 (d, J = 6 Hz, 72H, Me); ^{207}Pb NMR, δ 2482.

Synthesis of $[PbNb_2O(OPr^i)_{10}]_m$

Lead iodide (1.12 g, 2.42 mmol) was added to a suspension of $KNb(OPr^i)_6$ (2.36 g, 4.85 mmol) in 25 ml of toluene. After stirring at room temperature for *ca.* 4 h, refluxing was carried out for 12 h. Potassium iodide was separated by filtration. Cooling of the filtrate at −30 °C afforded large platelets (1.7 g, 70%), soluble in toluene and isopropyl alcohol. Anal. Calc. for $C_{30}H_{70}Nb_2O_{11}Pb$: C, 36.03; H, 7.00; Nb, 18.59; Pb, 20.74. Found: C, 35.35; H, 6.77; Nb, 17.90; Pb, 21.05%. IR (cm^{-1}): 1169m, 1135m, 1122s, 1025m, 998s, 984m, 955s; 852m, 829m, 800w, 771w, 721w; 577vs, 461m (νM−OR). ^{1}H NMR ($CDCl_3$), δ 5.00, 4.77, 4.65 (spt, J = 6 Hz, 7:2:1, 10H, CH), 1.33, 1.31 (d, J = 6 Hz, 60H, Me); $^{13}C\{^1H\}$ NMR ($CDCl_3$), δ 75.2 (CH), 26.1, 25.1, 22.9 (CH_3).

The same product was obtained by reacting $[Pb(OPr^i)_2]_\infty$ and $Nb(OPr^i)_5$ in toluene at room temperature.

Synthesis of $PbMgNb_2O(OAc)_2(OPr^i)_{10}$

$[Pb(OPr^i)_2]_\infty$ (0.87 g, 2.67 mmol) was added to a solution of $MgNb_2(OAc)_2(OPr^i)_{10}$ (1.76 g, 1.91 mmol) in 32 ml of a mixture of hexane–toluene (15:1). After stirring for 20 h at room temperature, the excess of lead isopropoxide was removed by filtration; crystallization of **5** as thin needles occurred at −30 °C (1.25 g, 57.3%). Anal. Calc. for $C_{34}H_{76}O_{15}MgNb_2Pb$: C, 35.76; H, 6.71; Mg, 2.13; Nb, 16.27; Pb, 18.14. Found: C, 35.53; H, 6.58; Mg, 2.5; Nb, 16.20; Pb, 18.07%. IR(cm^{-1}): 1605vs, 1582vs, ($\nu_{as}CO_2$); 1428s (ν_sCO_2); 1329m, 1260w, 1161vs, 1125vs, 1017vs, 998vs, 969vs, 953(sh), 899m, 847m, 836m, 828(sh), 667m; 604s, 580s, 560vs, 516m, 500m, 467m, 425m, 415m, 314m, 291m (νM−OAc, νMOR). ^{1}H NMR ($CDCl_3$), δ 4.75, 4.67, 4.54 (spt, J = 6.1 Hz, 4:4:2; 10H, CH), 1.9 (s, 6H, CH_3, OAc), 1.35, 1.30, 1.20 (d, J = 6.1 Hz, 4:4:2, 60H, CH_3); $^{13}C\{^1H\}$ NMR ($CDCl_3$), δ 177.5 (CO, Ac), 75.7, 75.5, 72.9, 71.9, 70.7 (CH), 26.7, 25.5, 25.2, 24.7, 24.3 (CH_3, Pr^i). ^{207}Pb NMR (C_7D_8), δ 4323.

Structure determination of $MgNb_2(OAc)_2(OPr^i)_{10}\cdot 0.5C_7H_8$

The selected crystal was mounted on a Enraf-Nonius CAD-4 automatic diffractometer. The unit-cell parameters and basic information about data collection at −100 °C and structure refinement are given in Table 2. Lattice parameters and orientation matrices were obtained from least-squares refinement of the setting angles of 25 well centred reflections in the range $6 < 2\theta < 35°$. The intensities of three standard reflections monitored every hour showed no decay. Corrections for Lorentz and polarization effects were applied.

Computations were performed using the PC version of CRYSTALS.[11] Scattering factors and corrections for anomalous dispersion were taken from ref. 12. The structure was solved using direct methods (SHELXS)[13] and standard Fourier techniques. One of the isopropyl groups [on O(11)] showed relatively large thermal parameters compared with the others. A best solution was found by the introduction of two disordered carbon atoms [C(23) and C(231)] each with half occupancy. All non-hydrogen atoms, except the two disordered carbon atoms, were refined anisotropically. A difference Fourier map showed the presence of a toluene molecule located on the C_2 axis, leading to the given complete formula. The very large values of the thermal parameters for this molecule suggests a disorder around the C_2 axis which could not be solved.

Atomic coordinates, thermal parameters, and bond lengths and angles have been deposited at the Cambridge Crystallographic Data Centre (CCDC). See Information for Authors, *J. Mater. Chem.*, 1997, Issue 1. Any request to the CCDC for this material should quote the full literature citation and the reference number 1145/47.

Results and Discussion

Synthesis

We have investigated the reactions between anhydrous metal acetates $M(OAc)_2$ (M = Mg, Ba, Cd, Pb) and niobium, namely

Table 2 Crystallographic data for $MgNb_2(OAc)_2(OPr^i)_{10}\cdot 0.5C_7H_8$ at −100 °C

M_w	965.1
a/Å	21.238(5)
b/Å	10.127(10)
c/Å	24.861(3)
α/°	90
β/°	107.77(2)
γ/°	90
V/Å^3	5110(5)
Z	4
crystal system	monoclinic
space group	$P2_1/c$
linear absorption coefficient μ/cm^{-1}	4.9
density ρ/g cm^{-3}	1.26
diffractometer	CAD4 Enraf-Nonius
radiation	Mo-Kα (0.71069)
scan type	ω–2θ
scan range/°	0.80 + 0.345 tan θ
θ limits/°	2–20
octants collected (*hkl*)	h 0–20, k 0–9, l −23 to 23
no. of data collected	4940
no. of unique data collected	4761
no. of unique data used for refinement	2891 [$(F_o)^2 > 3\sigma(F_o)^2$]
R_{int}	0.034
$R = \Sigma\|\|F_o\| - \|F_c\|\|/\Sigma\|F_o\|$	0.0544
$R_w = [\Sigma w(\|F_o\| - \|F_c\|)^2/\Sigma w F_o^2]^{1/2}$	0.0656(w = 1.0)
extinction parameter	0
goodness of fit, s	3.9
no. of variables	496
$\Delta\rho_{min,max}$/e Å^{-3}	−0.30, 0.38

ethoxide and isopropoxide. The choice of these systems was motivated by the attractive properties of niobates and tantalates as electrooptical ceramics [$LiNbO_3$, $(Sr,Ba)Nb_2O_6$ (SBN), $(Pb,La)(Ti,Nb)O_3$ (BLNT), $Pb(Sc,Nb)O_3$ (PSN)],[14] as ceramics for microwave resonators [$PbMg_{1/3}Nb_{2/3}O_3$ (PNM), $BaZn_{1/3}Ta_{2/3}O_3$ (BZT), $BaMg_{1/3}Ta_{2/3}O_3$ (BMT)],[15,16] or as dielectric ceramics ($CdNb_2O_6$).[5] Metal acetates are the most common precursors associated with metal alkoxides. Among the various coordination modes of the acetate ligand, the assembling ones (bridging or bridging–chelating) are generally favored, this suggests that carboxylates could be a means of maintaining the stoichiometry along the various steps through the hydrolysis–polycondensation process. These characteristics, which have been exploited for the formation of gels or fibers,[17] are however less attractive for MOCVD purposes.[18]

Reactions between metal alkoxides and carboxylates have generally been considered to proceed by elimination of an ester as a volatile byproduct, thus giving oxo derivatives. However, such reactions can occur in very mild conditions (room temperature and non-polar solvents), giving compounds whose formulation results from a simple addition. The reactions between divalent metal acetates of magnesium, cadmium and lead, and niobium isopropoxide, illustrate these features. These reactions proceed smoothly and quantitatively in hydrocarbons over 1 or 2 h, with progressive dissolution of the acetate according to eqn. (1). The excess of metal acetates is easily removed by filtration, while the novel compounds are crystallized out almost quantitatively from the filtrate.

$$M(OAc)_2 + 2Nb(OPr^i)_5 \xrightarrow[M = Mg\ \mathbf{1},\ Cd\ \mathbf{2},\ Pb\ \mathbf{3a}]{\text{hexane, } 25\,^\circ C} MNb_2(OAc)_2(OPr^i)_{10}$$

The $\nu_{as}CO_2$ stretching frequencies of the carboxylate ligands in the resulting complexes $MNb_2(OAc)_2(OPr^i)_{10}$ are generally shifted to higher frequencies with respect to those of the homometallic acetates (Table 1). This shift excludes the formation of mixed crystals $M(OAc)_2{,}2Nb(OPr^i)_5$. The difference $\Delta = \nu_{as}CO_2 - \nu_sCO_2$ suggests a chelating or bridging–chelating behavior for the OAc ligands.[19]

While the reactions between niobium isopropoxide and cadmium, magnesium or lead acetates occur easily, different behaviors are observed in the case of barium and of zinc. Scheme 1 summarizes the various routes investigated for access to Nb–M^{II} species (M = Mg, Ba, Zn, Cd, Pb). Barium acetate is inert toward $Nb(OR)_5$, even by heating in the presence of the parent alcool. The poor reactivity of barium acetate, which is actually a polymer based on tetranuclear units, is generally overcome by adding acetic acid,[20] but we observed no dissolution even in refluxing conditions by adding variable amounts of AcOH (up to 17 equivalents per Ba, this amount leading to gelification). A $BaNb_2(OPr^i)_{12}(Pr^iOH)_2$ species, obtained either by mixing the isopropoxides or by metathesis reaction between BaI_2 and $KNb(OPr^i)_6$, provides an alternative 'single-source' precursor for Ba–Nb materials.[8] Anhydrous zinc acetate is actually a soluble oxide acetate $Zn_4O(OAc)_6$, its reaction with $Nb(OPr^i)_5$ is thus more difficult to control and less selective than for the other divalent metal acetates as shown by the several $\nu_{as}CO_2$ absorption bands (1590, 1577, 1515 cm^{-1}). With the exception of the barium acetate, the anhydrous acetates of divalent metals $M(OAc)_2$ (M = Mg, Cd, Pb) are more reactive than these based on lanthanides since heating was required for the latter.[21]

The importance of the solvent on the formation of mixed-metal acetatoalkoxides is noteworthy. Whereas the reaction between $Cd(OAc)_2$ and $Nb(OPr^i)_5$ proceeds at room temperature, no reaction is observed with $[Nb(OEt)_5]_2$, even in refluxing toluene. Addition of small amounts of ethanol allows the reaction to proceed, probably as a result of the formation of the $Nb(OEt)_5(EtOH)$ monomer; $CdNb_2(OAc)_2(OEt)_{10}$ is thus obtained.[5] The $Pb(OAc)_2$–$Nb_2(OEt)_{10}$ system is more reactive than the $Cd(OAc)_2$–$Nb_2(OEt)_{10}$ system; $PbNb_2(OAc)_2(OEt)_{10}$ **3b** is obtained in toluene, under conditions similar to these of the isopropoxide analog, **3a**. The choice of a polar solvent which might act as a ligand toward $M(OAc)_2$ can be an unfavorable feature for complexation by a metal alkoxide. By contrast with hydrocarbons, no reaction occurs between $Pb(OAc)_2$ and $Nb(OEt)_5$ (1:2 stoichiometry) in THF, although solubilization of the acetate is achieved. ^{207}Pb NMR, which is a quite convenient tool [$I = 1/2$, sensitivity = 20.6%, wide range ($\approx$10 000 ppm of chemical shift)][22] for the analysis of the solutions of lead derivatives, only shows the presence of complexed lead acetate ($\delta = 2230$). One can notice that whereas $Pb_6O_4(OEt)_4$ reacts with $Nb(OEt)_5$ to form $Pb_6(\mu_4\text{-}O)_4(\mu_3\text{-}OEt)_4Nb_4(OEt)_{20}$,[23] the use of $Pb(OAc)_2$ as the source of lead oxide allows to acceed to precursors having a different Pb–Nb stoichiometry and thus to expand the range of 'single-source' precursors available for Nb–Pb oxide materials.

The new species are soluble in common organic solvents, thus allowing their characterization by NMR. All compounds **1**, **2**, **3a**, **3b** are fluxional, the exchange rate being dependent upon the size of the central nucleus. The exchanges between the different types of alkoxide ligands are frozen out already at room temperature for **1** while lower temperatures (−50 °C) are necessary for **2**, **3a** and **3b**. The acetate ligands are observed as a unique peak in the ^1H NMR spectra whereas the alkoxide signals appear as three resonances in a 2:2:1 ratio. The acetate ligands act as clips between the different metals and the solid-state structure is retained upon dissolution in non-polar as well as polar solvents. This is also confirmed by the NMR of the other nuclei (^{13}C, ^{207}Pb, ^{113}Cd).

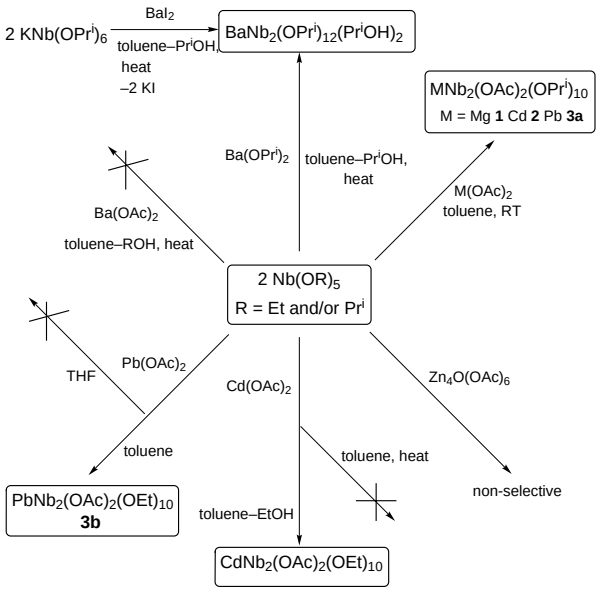

Scheme 1 Various routes to Nb–M^{II} species (M = Mg, Ba, Cd, Pb)

Molecular structures of $Nb_2M(\mu\text{-}OAc)_2(\mu\text{-}OPr^i)_4(OPr^i)_6$

The connectivity between the different metals has been established for the magnesium and cadmium derivatives by a single-crystal X-ray structure determination. Selected bond lengths and angles are collected in Table 3 for **1** and in Table 4 for **2**; the molecular structure of $MgNb_2(OAc)_2(OPr^i)_{10}$ is displayed in Fig. 1. The structure is related to that of $CdNb_2(OAc)_2(OPr^i)_{10}$. These trinuclear species display a bent, open-shell structure (Nb—Mg—Nb 139.45° for **1**), with alternating Nb and M atoms, all metal atoms being six-coordinate. The Nb—O bond distances span the range

Table 3 Selected bond distances (Å) and angles (degrees) for $MgNb_2(\mu\text{-}OAc)_2(\mu\text{-}OPr^i)_4(OPr^i)_6\cdot 0.5C_6H_5CH_3$ **1**

Mg(1)—O(1)	2.042(9)	Mg(1)—O(3)	2.044(5)	Nb(1)—O(10)	1.872(8)	Nb(1)—O(11)	1.879(8)
Mg(1)—O(5)	2.096(4)	Mg(1)—O(6)	2.093(8)	Nb(2)—O(2)	2.177(8)	Nb(2)—O(5)	2.012(7)
Mg(1)—O(7)	2.081(8)	Mg(1)—O(8)	2.080(9)	Nb(2)—O(7)	2.027(5)	Nb(2)—O(12)	1.878(8)
Nb(1)—O(4)	2.175(6)	Nb(1)—O(6)	2.025(7)	Nb(2)—O(13)	1.882(8)	Nb(2)—O(14)	1.877(7)
Nb(1)—O(8)	2.012(7)	Nb(1)—O(9)	1.878(6)	Mg(1)···Nb(1)	3.203(4)	Mg(1)···Nb(2)	3.194(3)
O(3)—Mg(1)—O(1)	90.9(3)	O(5)—Mg(1)—O(1)	89.0(3)	O(10)—Nb(1)—O(9)	96.0(3)	O(11)—Nb(1)—O(4)	84.4(3)
O(5)—Mg(1)—O(3)	168.3(3)	O(6)—Mg(1)—O(1)	93.7(3)	O(11)—Nb(1)—O(6)	165.3(4)	O(11)—Nb(1)—O(8)	92.5(4)
O(6)—Mg(1)—O(3)	90.5(3)	O(6)—Mg(1)—O(5)	101.2(3)	O(11)—Nb(1)—O(9)	95.9(4)	O(11)—Nb(1)—O(10)	95.0(4)
O(7)—Mg(1)—O(1)	89.7(3)	O(7)—Mg(1)—O(3)	93.6(3)	O(5)—Nb(2)—O(2)	85.5(3)	O(7)—Nb(2)—O(2)	83.3(3)
O(7)—Mg(1)—O(5)	74.7(3)	O(7)—Mg(1)—O(6)	174.7(3)	O(7)—Nb(2)—O(5)	77.7(3)	O(12)—Nb(2)—O(2)	85.8(3)
O(8)—Mg(1)—O(1)	167.1(4)	O(8)—Mg(1)—O(3)	90.5(3)	O(12)—Nb(2)—O(5)	168.5(3)	O(12)—Nb(2)—O(7)	93.7(3)
O(8)—Mg(1)—O(5)	92.1(3)	O(8)—Mg(1)—O(6)	73.5(3)	O(13)—Nb(2)—O(2)	178.4(2)	O(13)—Nb(2)—O(5)	93.8(3)
O(8)—Mg(1)—O(7)	103.0(3)	O(6)—Nb(1)—O(4)	85.2(3)	O(13)—Nb(2)—O(7)	95.2(3)	O(13)—Nb(2)—O(12)	94.8(4)
O(8)—Nb(1)—O(4)	85.7(3)	O(8)—Nb(1)—O(6)	76.4(3)	O(14)—Nb(2)—O(2)	84.7(3)	O(14)—Nb(2)—O(5)	93.3(3)
O(9)—Nb(1)—O(4)	179.6(3)	O(9)—Nb(1)—O(6)	94.5(3)	O(14)—Nb(2)—O(7)	165.5(3)	O(14)—Nb(2)—O(12)	93.4(3)
O(9)—Nb(1)—O(8)	94.1(3)	O(10)—Nb(1)—O(4)	84.2(3)	O(14)—Nb(2)—O(13)	96.8(3)		
O(10)—Nb(1)—O(6)	94.2(3)	O(10)—Nb(1)—O(8)	166.8(3)				
Nb(1)—O(6)—Mg(1)	102.2(3)	Nb(2)—O(5)—Mg(1)	102.0(3)	Nb(1)—O(8)—Mg(1)	103.1(3)	Nb(2)—O(7)—Mg(1)	102.0(3)
C(1)—O(2)—Nb(2)	130.4(7)	C(14)—O(8)—Nb(1)	136.5(8)	C(26)—O(12)—Nb(2)	163.7(13)	C(5)—O(5)—Mg(1)	120.50
C(3)—O(4)—Nb(1)	130.9(5)	C(20)—O(10)—Nb(1)	163.2(12)	C(32)—O(14)—Nb(2)	163.6(11)	C(8)—O(6)—Mg(1)	121.4(7)
C(8)—O(6)—Nb(1)	134.8(6)	C(23)—O(11)—Nb(1)	168.8(11)	C(29)—O(13)—Nb(2)	145.4(11)	C(11)—O(7)—Mg(1)	121.8(5)
C(17)—O(9)—Nb(1)	147.2(9)	C(5)—O(5)—Nb(2)	136.8(4)	C(1)—O(1)—Mg(1)	128.2(7)	C(14)—O(8)—Mg(1)	120.4(8)
C(23)—O(11)—Nb(1)	142.7(10)	C(11)—O(7)—Nb(2)	135.0(6)	C(3)—O(3)—Mg(1)	128.1(7)		

1.872(8)–2.175(6) Å for **1** and vary according to Nb—OR(t) < Nb—μ-OR < Nb—OAc. The magnesium–oxygen distances spread over the range 2.042(9)–2.096(4) Å; the Mg—OAc distances are slightly shorter than the Mg—OR ones. These data are in accord with the observations made on $CdNb_2(\mu\text{-}OAc)_2(OPr^i)_{10}$.[5] The non-bonding Mg···Nb distances are 3.369(8) Å(av.) and thus reflect the smaller size of the central metal as compared to the Cd–Nb species. The π character of the terminal Nb—OR bonds, a feature commonly observed for early transition metals,[24] is evidenced by the short Nb—O bond distances [1.88 Å (av.)] as well as by the large Nb—O—C angles, 164.8(12)° (av.) and 144.1(10)° (av.) for the equatorial and for the apical Nb—OR linkages, respectively. The various metals are six-coordinate but display a distorted surrounding, the distortion is the most severe for the central metal, magnesium, with O—Mg—O angles ranging from 73.5(3) to 168.3(3)°. The distortion of the central atom toward a trigonal prismatic surrounding has also been observed for the related heterometallic species $CdNb_2(\mu\text{-}OAc)_2(\mu\text{-}OPr^i)_4(OPr^i)_6$ (Table 4) and $BaNb_2(\mu\text{-}OPr^i)_4(OPr^i)_8(Pr^iOH)_2$.[8]

Reactivity

The reactivity of the mixed-metal acetatoalkoxides has been investigated (Scheme 2). Compounds **1** and **2** are quite stable with respect to further condensation by elimination of ester and no evolution is detected after *ca.* 20 h in refluxing toluene. The behavior of the lead system is more complex. In the case of **3a**, FTIR monitoring has shown the formation of isopropylacetate ($\nu_{as}CO_2 = 1745\ cm^{-1}$) during heating along with that of a new metallic derivative **4**, characterized by $\nu_{as}CO_2 = 1586\ cm^{-1}$ (the absorption bands corresponding to **3a** progressively decrease); **4**, analyzing as $Pb_2Nb_4O_5(OAc)_2(OPr^i)_{12}$, is more soluble than **3a** probably as a result of a close structure with peripheral organic groups. Its crystallization could be achieved in the presence of isopropyl alcohol. Unfortunately, the thin needles obtained were unsuitable for single-crystal X-ray diffraction studies. Low-temperature ^1H NMR data indicate three types of OR groups in a 4:4:4 integration ratio and one type of acetate ligand. A structure of type A is in accord with the overall spectroscopic data. The overall framework is related to that of the structurally characterized Ta–Zn oxoisopropoxide, $Ta_4Zn_2(\mu_3\text{-}O)_2(\mu\text{-}O)_2I_2(\mu\text{-}OPr^i)_6(OPr^i)_8$.[25] Similar observations, formation of different species if the reaction is performed at room temperature or at reflux were reported by us for the $Pb(OAc)_2$–$Ti(OPr^i)_4$ system although the species obtained differed more in their solubility properties.[26] In contrast to **3a**, the oxoacetatoalkoxide $Pb_2Ti_2O(OAc)_2(OPr^i)_8$, obtained at room temperature, is not modified by further heating, probably because the metals are already assembled by an oxo ligand.

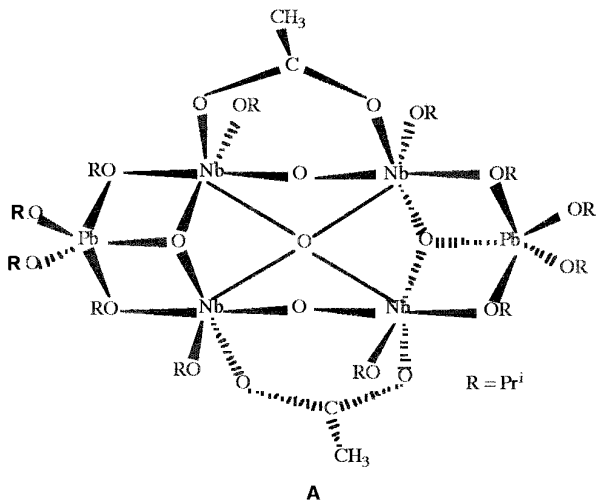

A

Significant differences were found if the reaction between $Nb(OPr^i)_5$ and $Pb(OAc)_2$ (1:1 stoichiometry) was performed in refluxing toluene instead of at room temperature: the formation of another oxoacetatoalkoxide **5** is observed. In contrast to **4**, **5** is poorly soluble, the presence of broad absorptions bands in the range 800–650 cm^{-1} in its FTIR spectrum suggests extended Nb—O—Nb bonds and thus a polymeric nature.[27] Compound **5** also displays absorption bands characteristic of $\nu_{as}CO_2$ and ν_sCO_2 vibrations at 1547 and 1401 cm^{-1} respectively. These results may explain the evolution of the solubility over time reported in the literature by refluxing $Pb(OAc)_2$ and $Nb(OEt)_5$ in the course of the

Table 4 Selected bond lengths (Å) and angles (degrees) for $Nb_2Cd(\mu\text{-}OPr^i)_4(\mu\text{-}OAc)_2(OPr^i)_6$ **2**

Cd(1)—Nb(1)	3.3820(8)	Cd(1)—Nb(2)	3.3962(8)	Nb(1)—O(8)	1.991(4)	Nb(1)—O(9)	1.878(4)
Cd(1)—O(1)	2.260(4)	Cd(1)—O(3)(2)	2.270(4)	Nb(1)—O(10)	1.877(4)	Nb(1)—O(11)	1.882(4)
Cd(1)—O(5)	2.291(4)	Cd(1)—O(6)	2.312(4)	Nb(2)—O(2)	2.169(4)	Nb(2)—O(5)	2.008(4)
Cd(1)—O(7)	2.332(4)	Cd(1)—O(8)	2.313(4)	Nb(2)—O(7)	2.003(4)	Nb(2)—O(12)	1.876(4)
Nb(1)—O(4)	2.167(4)	Nb(1)—O(6)	2.025(4)	Nb(2)—O(13)	1.887(4)	Nb(2)—O(14)	1.876(4)
O(5)—Cd(1)—O(1)	88.2(2)	O(5)—Cd(1)—O(3)	159.7(2)	O(7)—Cd(1)—O(6)	116.2(1)	O(8)—Cd(1)—O(6)	68.4(1)
O(6)—Cd(1)—O(1)	159.1(1)	O(6)—Cd(1)—O(3)	86.4(2)	O(7)—Cd(1)—O(5)	68.3(1)	O(8)—Cd(1)—O(5)	110.4(1)
O(6)—Cd(1)—O(5)	97.2(1)	O(8)—Cd(1)—O(1)	90.8(1)	O(7)—Cd(1)—O(6)	116.2(1)	O(8)—Cd(1)—O(7)	175.2(1)
O(7)—Cd(1)—O(3)	92.1(1)	O(8)—Cd(1)—O(3)	89.6(2)				
O(6)—Nb(1)—O(4)	82.6(2)	O(7)—Nb(2)—O(5)	80.6(2)	O(10)—Nb(1)—O(8)	170.0(2)	O(14)—Nb(2)—O(2)	84.1(2)
O(8)—Nb(1)—O(4)	87.9(2)	O(12)—Nb(2)—O(2)	86.0(2)	O(11)—Nb(1)—O(6)	166.1(2)	O(14)—Nb(2)—O(7)	164.9(2)
O(9)—Nb(1)—O(6)	95.2(2)	O(12)—Nb(2)—O(7)	93.7(2)	O(11)—Nb(1)—O(9)	97.8(2)	O(14)—Nb(2)—O(13)	96.3(2)
O(10)—Nb(1)—O(6)	90.8(2)	O(13)—Nb(2)—O(2)	179.4(2)	Nb(1)—O(6)—CD(1)	102.3(2)	Nb(2)—O(5)—CD(1)	104.2(2)
O(10)—Nb(1)—O(9)	93.2(2)	O(13)—Nb(2)—O(7)	96.1(2)	Nb(1)—O(8)—CD(1)	103.3(2)	Nb(2)—O(7)—CD(1)	102.9(2)
O(11)—Nb(1)—O(4)	84.4(2)	O(14)—Nb(2)—O(5)	90.2(2)	Nb(1)—O(4)—C(3)	138.8(4)	Nb(2)—O(2)—C(1)	137.2(4)
O(11)—Nb(1)—O(8)	94.0(2)	O(14)—Nb(2)—O(12)	93.8(2)	Nb(1)—O(6)—C(8)	127.2(4)	Nb(2)—O(5)—C(5)	127.8(4)
O(11)—Nb(1)—O(10)	93.1(2)	O(5)—Nb(2)—O(2)	86.1(2)	Nb(1)—O(8)—C(14)	137.0(4)	Nb(2)—O(7)—C(11)	137.2(4)
O(8)—Nb(1)—O(6)	80.7(2)	O(7)—Nb(2)—O(2)	83.4(2)	Nb(1)—O(9)—C(17)	137.0(5)	Nb(2)—O(12)—C(26)	167.5(5)
O(9)—Nb(1)—O(4)	177.6(2)	O(12)—Nb(2)—O(5)	170.7(2)	Nb(1)—O(10)—C(20)	150.9(5)	Nb(2)—O(13)—C(29)	141.7(5)
O(9)—Nb(1)—O(8)	92.7(2)	O(13)—Nb(2)—O(5)	93.5(2)	Nb(1)—O(11)—C(23)	155.6(4)	Nb(2)—O(14)—C(32)	153.6(5)
O(10)—Nb(1)—O(4)	85.8(2)	O(13)—Nb(2)—O(12)	94.4(2)				

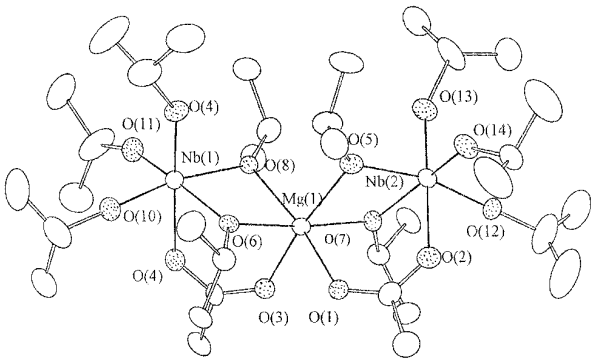

Fig. 1 Molecular structure of $MgNb_2(\mu\text{-}OAc)_2(\mu\text{-}OPr^i)_4(OPr^i)_6$ showing the atom numbering scheme (ellipsoids at 20% probability)

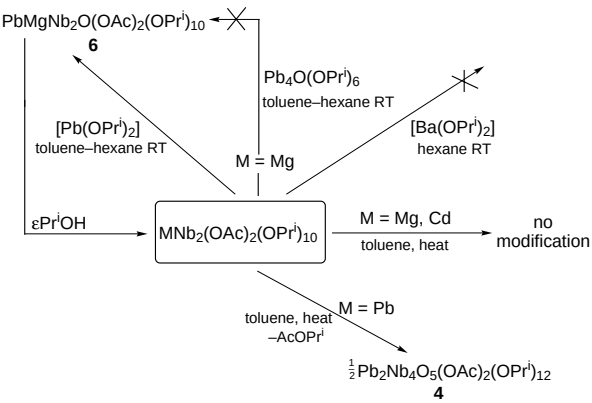

Scheme 2 Reactivity of the $MNb_2(OAc)_2(OPr^i)_{10}$ (M = Mg, Cd, Pb) species

preparation of a PNM ceramic.[28] Allowing the formation of the mixed-metal species to proceed, prior to heating, can be crucial for the homogeneity of the system.

Terheterometallic alkoxides have been reported recently.[29] The reactivity of some of the heterometallic species toward other metal complexes has been estimated. In view of the formulation of ternary oxides, $MgNb_2(OAc)_2(OPr^i)_{10}$ **1** seemed to be a good candidate for such investigations. No reaction was observed between **1** and $[Ba(OPr^i)_2]_\infty$ or $Pb_4O(OPr^i)_6$ at room temperature, even after two days. The polymeric lead isopropoxide was more reactive and its dissolution was observed at room temperature in toluene, ^{207}Pb NMR spectroscopy was used to get some insight into the molecular composition of the reaction medium. Several signals are detected (δ 4323, 3838, 3803 and 2591). The predominant species, characterized by the chemical shift at δ 4323, could be isolated by crystallization (57% yield) and contains niobium, magnesium and lead. Analytical data imply the empirical formula $PbMgNb_2O(OAc)_2(OPr^i)_{10}$ **6**. The proton NMR spectrum at room temperature indicates the presence of three types of methine groups in an integration ratio 4:4:2. Low-temperature spectra show a broadening but give no additional information. ^{13}C NMR spectra however show five types of methine groups. The overall NMR data (^{1}H, ^{13}C and ^{207}Pb NMR) are in accord with a structure of type B. This structure, in which all metals display their usual coordination numbers, namely six for magnesium and niobium, and five for lead, can be viewed as the association between **1** and a PbO moiety. It is also supported by the facile dissociation of **6** in the presence of trace amounts of isopropyl alcohol to give **1**.

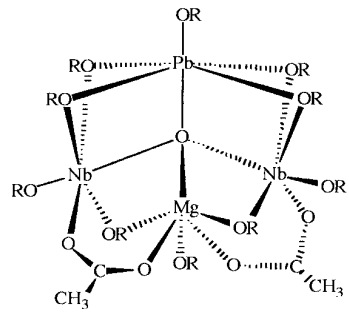

B

The reactivity of $BaNb_2(OPr^i)_{12}(Pr^iOH)_2$ **7** was also considered (Scheme 3). Attempts to control its hydrolysis by adding acetic acid in toluene at room temperature offered poorly soluble species, one of them having being identified as $Nb_4O_4(\mu\text{-}OAc)_4(OPr^i)_8$ (ν_sCO_2 1591, νM—OR 489, 410 cm^{-1}) by comparison with an authentic sample.[30] The reaction between **7** and lead acetate is governed by redistribution phenomena with extrusion of barium as barium acetate and formation of a Nb–Pb isopropoxide derivative, $[PbNb_2O(OPr^i)_{10}]_m$ **8**, which was identified by comparison with an authentic sample obtained more directly by reacting lead iodide and $KNb(OPr^i)_6$.

$BaNb_2(OPr^i)_{12}(Pr^iOH)_2$ displays two solvating alcohol molecules, these may act as functional ligands since their acidity is enhanced by coordination thus allowing their reactivity toward labile metallic species.[4,31] Trimethylsilylamides are attractive candidates for the introduction of another metal, the by-product being the volatile amine $HN(SiMe_3)_2$. Zinc trimethylsilylamide however was found to be inert toward $BaNb_2(OPr^i)_{12}(Pr^iOH)_2$ at room temperature in hexane. Heating promotes a reaction but zinc separates out from the reaction medium as insoluble zinc isopropoxide and the initial Ba–Nb species is recovered by adding isopropyl alcohol. Lead trimethylsilylamide $Pb[N(SiMe_3)_2]_2$ is more reactive. Its reaction with **7** at room temperature is evidenced by the discoloration of the reaction medium as well as by the presence in the ^{207}Pb NMR spectrum of two species having chemical shifts different from lead isopropoxide derivatives known so far. The major species, which could be isolated, corresponds to a derivative **9** containing three metals, Ba, Nb and Pb, and characterized by a single peak at δ 4059 in its ^{207}Pb NMR spectrum. Attempts to obtain crystals suitable for X-ray diffraction studies were unsuccessful as a result of its poor stability. In the presence of small amounts of isopropyl alcohol, lead oxoisopropoxide, $Pb_4O(OPr^i)_6$, is obtained together with the initial Ba–Nb species **7**. The overall results indicate that terheterometallic species based on a combination of metals of interest for materials are quite difficult to stabilize and an

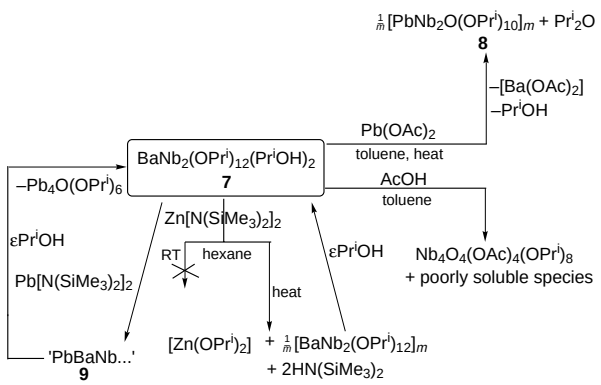

Scheme 3 Reactivity of $BaNb_2(OPr^i)_{12}(Pr^iOH)_2$ (εPr^iOH stands for small amount)

appropriate set of ligands is required as in the case of compound **6**.

Hydrolysis–condensation reactions

Hydrolysis–condensation reactions have been achieved for various hydrolysis ratios h [$h=[H_2O]/[MM'(OR)_{n+n'}]$ in THF or in the parent alcohol (0.1–0.01 M). Powders obtained for large excess of water ($h=30$) have been analyzed by FTIR, thermogravimetry (TG), differential thermal analysis (DTA) and X-ray diffraction (XRD) at various temperatures.

Ligands such as carboxylates or β-diketonates are expected to reduce the hydrolysis rates and to modify morphology and/or size of the particles.[14] The influence of the ancillary ligands on the properties of the final material can be estimated when mixed-metal species having the same MM′ stoichiometry but a different set of ligands are available. The Mg–Nb, Pb–Nb systems, discussed here, and the Pb–Ti system reported previously[26] offer such opportunities.

The influence of the ancillary ligand, OR *vs.* OAc, can be illustrated with the Pb–Nb system. As expected, differential hydrolysis is observed for the acetatoalkoxide derivatives and the powders resulting from the hydrolyses indicate residual carboxylate ligands ($\nu_{as}CO_2$ at 1572 and 1545 cm^{-1} for **1** and **3a** respectively). The hydrolysis of $PbNb_2(OAc)_2(OPr^i)_{10}$ in isopropyl alcohol (0.1 M) gives a homogeneous clear solution up to $h=5$. $PbNb_2(OAc)_2(OPr^i)_{10}$ remains actually inert toward the addition of water up to $h=2$ in isopropyl alcohol (FTIR and ^{207}Pb NMR). Fig. 2(*a*) shows representative TG and DTA curves for the powder derived from the hydrolysis (large hydrolysis ratios) of **3a**. A nearly continuous mass loss is observed between 80 and 420 °C. This indicates that the residual carboxylate ligands are burnt out at relative low temperatures. The DTA curve shows an exotherm around 600 °C suggesting the formation of a crystalline material. This is confirmed by XRD. The powders appear amorphous at room temperature but crystallize at 600 °C as the pure $PbNb_2O_6$ phase [Fig. 2(*b*)], traces of $PbNb_4O_{11}$ are observed at 800 °C as a result of some loss of lead oxide. By contrast to the smooth hydrolysis of $PbNb_2(OAc)_2(OPr^i)_{10}$, that of $[PbNb_2O(O^iPr)_{10}]_m$ **8** in isopropyl alcohol proceeds with immediate precipitation. The X-ray diffraction patterns after thermal treatment of the powder (obtained for $h=30$) show no $PbNb_2O_6$ but crystalline $Pb_3Nb_4O_{13}$ at 600 °C together with $PbNb_4O_{11}$ at 750 °C. These observations suggest that segregation between the metals occurs at the early stages of the hydrolysis–polycondensation process. This is also confirmed in the Mg–Nb–OR system.

$MgNb_2(OAc)_2(OPr^i)_{10}$ **1**, $MgNb_2(OEt)_{12}(EtOH)_2$ **10** and $MgNb_2(OPr^i)_{12}$ are all potential precursors of $MgNb_2O_6$. These molecules are fragments of a chain made up of three octahedra and are thus related to a multicomponent oxide which displays a columbite-type structure $[(NbO_6)(MO_6)(NbO_6)]_\infty$. Hydrolysis proceeds with the formation of amorphous powders in all cases. As for the powder derived from the hydrolysis of **3a**, the thermal elimination of the acetate ligand is complete below 500 °C for the powder derived from acetatoalkoxide **1** as precursor [Fig. 3(*a*)]. Crystallisation starts around 500 °C and the $MgNb_2O_6$ phase is obtained pure and well crystallized at 600 °C [Fig. 3(*b*)]. By contrast, the crystallization only starts at *ca.* 700 °C for the powder resulting from hydrolysis of **10** and quite high temperatures are required for the formation of the multicomponent oxide [Fig. 4(*b*)]. Partial retention of carboxylate ligands after the hydrolysis of **1**, as shown by FTIR, assists the build-up of an ordered, crystalline material. The formation of sols of nanosize particles over a large range of hydrolyses ratios (up to $h=24$) in isopropyl alcohol, which makes $MgNb_2(OPr^i)_{12}$ an interesting precursor for thin film applications, is however an unfavorable feature on account of crystallization and homogeneity. Light scattering measurements have shown that the sols are polydisperse [20 (88%) and 223 (12%) nm]. Electron dispersive X-ray analysis (EDAX) by transmission electron microscopy (TEM) indicate that the small particles are mixed-metal species (Mg:Nb 1:2) whereas larger particles result from metal segregation and more reorganization is thus necessary. Ceramics, such as for instance $CdNb_2O_6$ and $MgNb_2O_6$

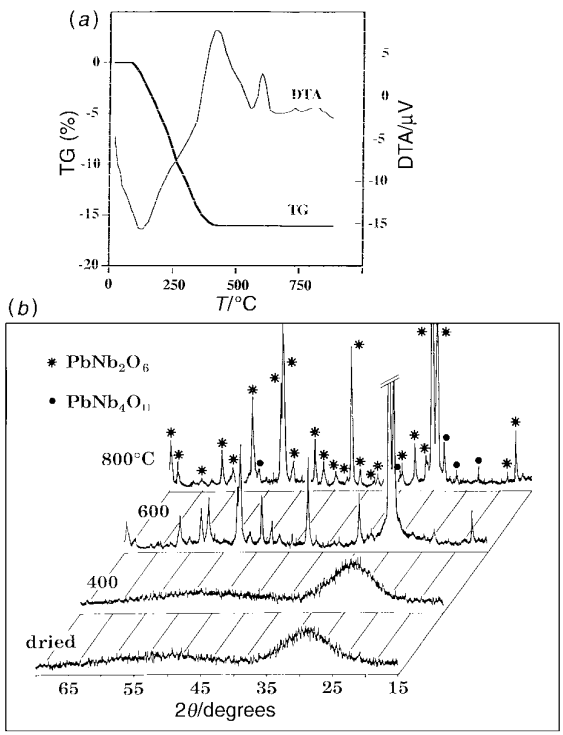

Fig. 2 TG profile (*a*) and XRD patterns at various temperatures (*b*) for the powder resulting from the hydrolysis of $PbNb_2(OAc)_2(OPr^i)_{10}$

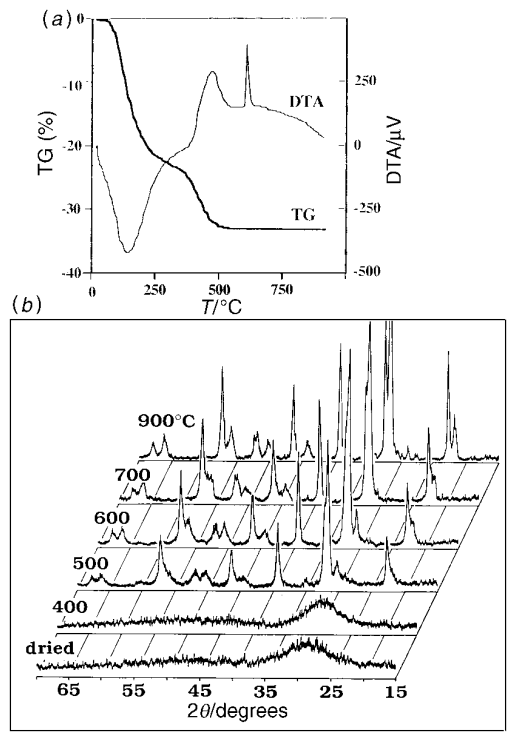

Fig. 3 TG profile (*a*) and XRD patterns at various temperatures (*b*) for the powder resulting from the hydrolysis of $MgNb_2(OAc)_2(OPr^i)_{10}$

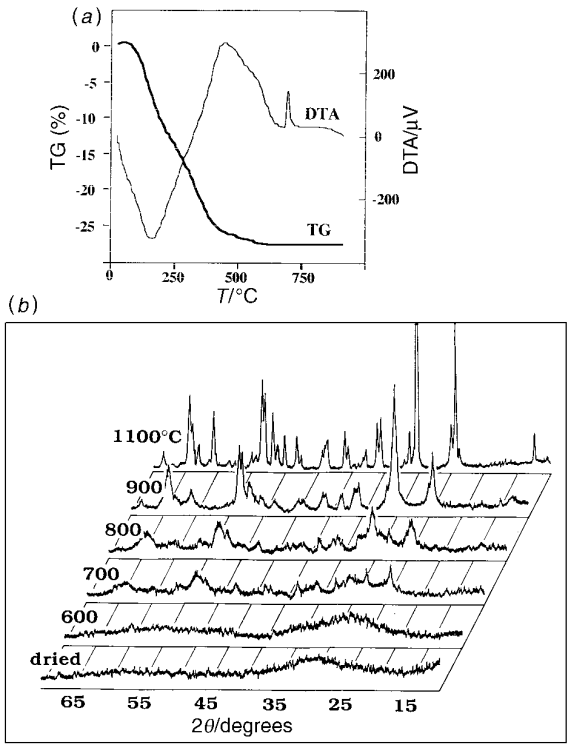

Fig. 4 TG profile (*a*) and XRD patterns at various temperatures (*b*) for the powder resulting from the hydrolysis of $MgNb_2(OPr^i)_{12}$

are already well crystallized at 600 °C, while temperatures >1000 °C are required for conventional routes.[32]

Conclusion

Mixed-metal acetatoalkoxides can be obtained readily by reacting niobium isopropoxide and anhydrous acetates $M(OAc)_2$ (M = Mg, Cd, Pb) at room temperature in non-polar solvents. The reactions are selective and proceed to the formation of the smallest aggregates which allow the metals to achieve their common coordination numbers regarding the steric demand of the alkoxide ligand. Niobium tends to be six-coordinate and this is possible *via* simple addition products. The experimental conditions, choice of solvent and temperature of the reaction are important in determining the reaction products. The system based on lead is the most reactive and condensation can be induced thermally. The acetate groups act always as assembling ligands as evidenced by the X-ray structural data and by the difference in the stretching frequencies $\nu_{as}CO_2 - \nu_s CO_2 < 200\ cm^{-1}$. It assists the building up of an ordered, crystalline material in the course of the hydrolysis–polycondensation process, thus favoring the formation of single-phase materials at quite low temperatures.

The authors are grateful to the CNRS (GRECO) for financial support and Dr F. Chaput (Ecole Polytechnique, Palaiseau) for powder X-ray diffraction experiments.

References

1 S. L. Swartz and V. E. Wood, *Condens. Matter News*, 1992, **1**, 4; G. H. Haertling, *Electroceramics*, ed. M. L. Levinson, M. Dekker, New York, 1988.
2 L. G. Hubert-Pfalzgraf, *Polyhedron*, 1994, **13**, 1181; *Mater. Res. Soc. Symp. Proc.*, 1992, **271**, 15.
3 C. D. Chandler, C. Roger and M. J. Hampden-Smith, *Chem. Rev.*, 1993, **93**, 1205.
4 K. G. Caulton and L. G. Hubert-Pfalzgraf, *Chem. Rev.*, 1990, **90**, 969.
5 S. Boulmaâz, R. Papiernik, L. G. Hubert-Pfalzgraf, J. C. Daran and J. Vaissermann, *Chem. Mater.*, 1991, **3**, 779.
6 D. C. Bradley, B. N. Chakravarti and W. Wardlaw, *J. Chem. Soc.*, 1956, 2381.
7 M. C. Massiani, R. Papiernik and L. G. Hubert-Pfalzgraf, *Polyhedron*, 1991, **10**, 1667; S. C. Goel, M. Y. Chiang and W. E. Buhro, *Inorg. Chem.*, 1990, **29**, 4640.
8 S. Boulmaâz, R. Papiernik, L. G. Hubert-Pfalzgraf and J. C. Daran, *Eur. J. Solid State Inorg. Chem.*, 1993, **30**, 583; E. P. Turevskaya, N. Ya Turova, A. V. Korolev, A. I. Yanovsky and Yu T. Struchkov, *Polyhedron*, 1995, **14**, 1531.
9 D. H. Harris and M. F. Lappert, *J. Chem. Soc., Chem. Commun.*, 1974, 895.
10 H. Burger, W. Sawodny and H. Wannaghat, *J. Organomet. Chem.*, 1965, **3**, 113.
11 D. J. Watkin, J. R. Carruthers and P. W. Betteridge, *Crystals User Guide*, Chemical Crystallography Laboratory, University of Oxford, Oxford, 1986.
12 D. T. Cromer, *International Tables for X-Ray Crystallography*, Kynoch Press, Birmingham, 1974, vol. 4.
13 G. M. Sheldrick, *SHELXS in Crystallographic Computing 3*, ed. G. M. Sheldrick, C. Kruger and R. Goddard, Oxford University Press, Oxford, 1985, p. 175.
14 L. G. Hubert-Pfalzgraf, *Chemical Processing of Ceramics*, ed. B. I. L. Lee and E. J. A. Pope, M. Dekker, New York, 1994, ch. 2, p. 23; M. I. Yanovskaya, E. P. Turevskaya, V. G. Kessler, I. E. Obvintseva and N. Ya. Turova, *Integrated Ferroelectrics*, 1992, **1**, 343.
15 F. Chaput, J. P. Boilot, M. Lejeune, R. Papiernik and L. G. Hubert-Pfalzgraf, *J. Am. Ceram. Soc.*, 1989, **72**, 1355.
16 O. Renoult, J. P. Boilot, F. Chaput, R. Papiernik, L. G. Hubert-Pfalzgraf and M. Lejeune, *Ceramics Today—Tomorrow's Ceramics*, Elsevier, London, 1991, p. 1991.
17 J. Livage, M. Henry and C. Sanchez, *Prog. Sol. State Chem.*, 1988, **18**, 259.
18 L. G. Hubert-Pfalzgraf, *Appl. Organomet. Chem.*, 1992, **6**, 627.
19 G. B. Deacon and R. J. Phillips, *Coord. Chem. Rev.*, 1980, **33**, 227.
20 A. Mosset, I. Gautier-Luncau, J. Galy, P. Strehlow and H. Schmidt, *J. Non-Cryst. Solids*, 1988, **100**, 339.
21 S. Daniele, L. G. Hubert-Pfalzgraf, J. C. Daran and R. Toscano, *Polyhedron*, 1993, **12**, 2091.
22 J. J. Dechter, *Prog. Inorg. Chem.*, 1982, **29**; R. K. Harris, J. J. Kennedy and W. McFarlane, *NMR and the Periodic Table*, ed. R. K. Harris and B. E. Mann, Academic Press, London, 1978.
23 R. Papiernik, L. G. Hubert-Pfalzgraf, J. C. Daran and Y. Jeannin, *J. Chem. Soc., Chem. Commun.*, 1990, 695.
24 M. H. Chisholm, *Chemtracts: Inorg. Chem.*, 1992, **4**, 273.
25 S. Boulmaaz, L. G. Hubert-Pfalzgraf, S. Halut and J. C. Daran, *J. Chem. Soc., Chem. Commun.*, 1994, 601.
26 S. Daniele, R. Papiernik, L. G. Hubert-Pfalzgraf, S. Jagner and M. Hakansson, *Inorg. Chem.*, 1995, **34**, 628; L. G. Hubert-Pfalzgraf, S. Daniele, R. Papiernik, M. C. Massiani, B. Septe, J. Vaissermann and J. C. Daran, *J. Mater. Chem.*, 1997, **7**, 753.
27 L. G. Hubert-Pfalzgraf, M. Postel and J. G. Riess, *Comprehensive Coordination Chemistry*, Pergamon Press, London, 1987, ch. 34.
28 T. Fukui, C. Sakurai and M. Okuyama, *J. Non Cryst. Solids*, 1991, **134**, 293.
29 M. Veith, S. Mathur and V. Huch, *J. Am. Chem. Soc.*, 1996, **118**, 903; M. Veith, S. Mathur and V. Huch, *J. Chem. Soc., Dalton Trans.*, 1996, 2485.
30 R. Papiernik, L. G. Hubert-Pfalzgraf and J. Vaissermann, to be published.
31 B. A. Vaarstra, J. C. Huffman, W. E. Streib and K. G. Caulton, *Inorg. Chem.*, 1991, **30**, 3068; V. G. Kessler, L. G. Hubert-Pfalzgraf, S. Halut and J. C. Daran, *J. Chem. Soc., Chem. Commun.*, 1994, 705.
32 *Gmelin, Handbuch der anorganische Chemie 'Vanadium, Niobium, Tantalum*,' Springer-Verlag, Berlin, 1973.

Paper 7/01381G; *Received* 27*th February*, 1997